Proceedings of the European Nuclear Young Generation Forum
ENYGF'21
September 27-30, 2021, Tarragona, Spain

Depth profiling of radiologically contaminated concrete using computed tomography images and Monte Carlo simulations

Brabants, Lowie[1*], Simons Mattias[1], Reniers, Brigitte[1], Paepen, Jan[2], Vandoren, Bram[3] and Schroeyers, Wouter[1]

[1] Hasselt University, NuTeC, CMK, Nuclear Technology - Faculty of Engineering Technology, Agoralaan building H, B-3590 Diepenbeek, Belgium; [2] European Commission, Joint Research Centre, Retieseweg 111, B-2440 Geel, Belgium; [3] Hasselt University, CERG, Faculty of Engineering Technology, Agoralaan building H, B-3590 Diepenbeek, Belgium

*Corresponding author: *lowie.brabants@uhasselt.be*

I. INTRODUCTION

Due to the ageing of the nuclear power plants (NPPs) in Europe, it is expected that during next decade more and more reactors will have to be decommissioned and dismantled [1]. This ageing trend can also be observed for the 7 operational reactors in Belgium. Three of the reactors finished construction in 1975. The other four reactors were commissioned between 1982 and 1985 which leads to an average age that exceeds 40 years. All of the reactors are planned to be closed by 2025, opening up the Belgian nuclear decommissioning market. For the decommissioning of these reactors, a "back to greenfield" strategy will be applied, meaning that the site of the NPPs will be brought back to the initial situation before the power plants were built [2].

For the decommissioning, an important factor that determines the total cost is the amount of generated radioactive waste. The approach will be to minimize the fraction of radioactive waste, by accurately performing radiological characterizations of the waste streams to separate non-radioactive waste streams from radioactive waste and by (where possible) decontamination of waste [3].

A frequently encountered waste stream is concrete as it is one of the most common material used in the construction of a NPP. Most concrete waste can be classified as conventional waste, but for concrete used in the containment building, radiological contamination is frequently encountered. To determine a correct decontamination strategy for this concrete, the first step is to perform radiological characterisations to quantify the nature of the contamination and its depth [4].

These characterisations can be destructive (by taking core drilling samples), but can also be performed by non-destructive in-situ measurements (see Figure 1). Core drilling samples are frequently used to determine the contamination depth. Concrete cores are extracted from structures, segmented, pulverized and characterized. Although this technique is accurate, it only provides information on the contamination depth at a very local level. The sample might not be representative for the surrounding material and as a result, a gross over or underestimation of the contamination depth may be present. Moreover, this technique is labour intensive (and thus costly) and may also lead to the spreading of contaminated dust [5], [6].

Figure 1. destructive core drilling procedure (left)[7]**, non-destructive radiological characterisation with handheld scintillator detector (right)**[8]

An alternative to destructive sampling are in-situ measurements. The most basic approach to determine contamination non-destructively is by using handheld equipment such as scintillator detectors. However, this technique is not only time consuming as scanning is performed manually, but the depth information is also limited to the superficial activity. As a result, multiple cycles of measurements and decontaminations are often performed before the desired residual activity levels are achieved [5], [9].

A more advanced non-destructive technique can be performed using the spectral information acquired with high-purity germanium (HPGe) detectors and to determine contamination characteristics such as activity levels, radionuclide inventory and contamination depths.

The depth profiling technique that is considered in this research is the relative linear attenuation (RLA) model. This method is applied to the relative intensities of the X-ray and gamma emissions of key radionuclide ^{137}Cs [10]. The model assumes an exponential decrease of the contamination as a

function of depth. Such profile has been frequently reported for contaminations in both an environmental and decommissioning context. The RLA model can be applied to determine the total activity of ^{137}Cs and the relaxation length RL (which is an important depth parameter) of the exponential contamination profile [7], [8], [12]. After determining these quantities, the decontamination plan, indicating the locations and depths of concrete to be removed, can be constructed.

Although the RLA technique has already been applied in a decommissioning context, this method still has its shortcomings as it assumes a perfect exponential function and a perfect homogeneous base material. Both of these assumptions are not completely applicable for concrete. Concrete is far from homogeneous as it consists out of a mixture of mortar, aggregates and voids. Furthermore, the contamination is observed to be more pronounced in the porous mortar phase of the concrete than in the aggregates [13], [14].

As the performance of a depth profiling technique directly influences the total amount of radioactive waste being generated, it is important to further optimize the existing techniques and quantify operational limits and error sources. In other words, having correct radiological information of the installation, even before the start of the decontamination process, is an upstream tool to directly limit the amount of radioactive waste being generated in a decommissioning project.

To study the performance of the RLA technique, a Monte Carlo (MC) model was constructed in this research consisting of a HPGe detector setup with contaminated concrete samples. A MC model is a computational method to study interactions of ionizing radiation with matter. The complexity of the concrete was incorporated into the model by making Computed Tomography (CT) images of the concrete in order to visualize the aggregates, mortar and voids. Different exponential profiles were then applied to the concrete model to quantify the error on the contamination activity (determined by the full-energy peak efficiency), and on the depth estimation (determined by the relaxation length) resulting from the RLA model.

II. HPGE MODEL

An extended-range coaxial p-type HPGe detector (type GX9023 from Mirion) was modelled and the performance of the resulting MC model was validated by comparing the full-energy peak (FEP) efficiency of the MC model to the experimentally determined FEP efficiency. The FEP efficiency is an important factor that links the area of a spectral peak directly to the activity of the source.

These measurements were performed with a variety of reference sources, measured at different source-to-endcap distances. The sources contained multiple radionuclides to validate the detector model over a broad energy range. The following sources were used:

- Point sources: ^{137}Cs, ^{134}Cs, ^{60}Co, ^{152}Eu and ^{241}Am;
- Volumetric water sources: ^{60}Co, ^{137}Cs, ^{134}Cs, ^{133}Ba and ^{152}Eu;
- Volumetric silicone-based sources: ^{139}Ce, ^{60}Co, ^{137}Cs, ^{113}Sn, ^{85}Sr, ^{57}Co, ^{51}Cr, ^{88}Y, ^{133}Ba, ^{109}Cd, ^{241}Am and ^{210}Pb.

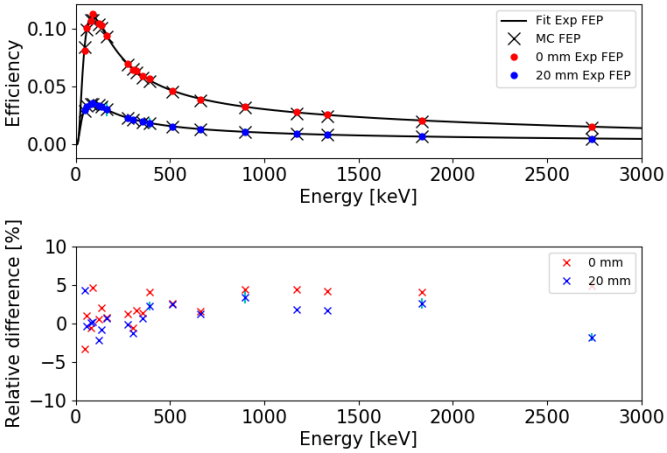

Figure 2. Experimental and MC calculated detector efficiencies for measurements of the volumetric silicone source at 0 mm and 40 mm from the detector endcap (top). The relative difference between the experimental and MC detector efficiencies (bottom) [15].

The MC model was considered to be validated when the relative difference of the model to the experimental data was in agreement considering an imposed criterion of 5% relative difference for gamma rays with an energy between 100 keV and 2000 keV and 10% relative difference for gamma or x-rays with energies lower than 100 keV or higher than 2000 keV. For each source, the model performed within these tolerance limits. Figure 2 shows the results of the MC model for the volumetric silicone source which was measured at 0 and 20 mm distance from the detector endcap [15].

III. CONCRETE MODEL

Different concrete samples containing limestone aggregates were made and used as the basis for the contamination measurements. After demoulding, the samples were cured for 21 days. In the next step, the samples were scanned with a CT-scanner (Philips Brilliance CT Big Bore). These CT images are then converted to a MC model to study the impact of the inhomogeneity of the concrete samples on the performance of the RLA model. As this model is based on the assumption of a completely homogeneous base material, it is expected that errors in depth estimations will be made when the method is applied to the complex matrix of concrete which consists of higher density aggregates, surrounded by mortar in which air cavities are also present (so-called voids).

As the casted concrete samples were not spiked with any radioactive ^{137}Cs, the contamination was simulated by incorporating multiple contamination profiles in the MC model. Different exponential equations are simulated on different concrete samples according to equation 1:

$$A(x) = A(0)e^{-x/RL} \quad (1)$$

Where A is the activity level [Bq] at the surface or at depth x [mm] and RL stands for the relaxation length [mm] which describes the slope of the activity decrease with depth. Simulated 1/RL values varied from 0 (representing a

completely uniform profile) to 1 (representing a steep exponentially decreasing contamination profile) [12].

Adding to this contamination profile, activity has also been shown to be more present in the porous mortar phase of the concrete rather than in the aggregates themselves [13], [14]. This aspect of selectivity of the contamination is also incorporated in the MC model, as no particles are generated within the volume occupied by the aggregates. Figure 3 represents the different steps that were performed to construct the MC model.

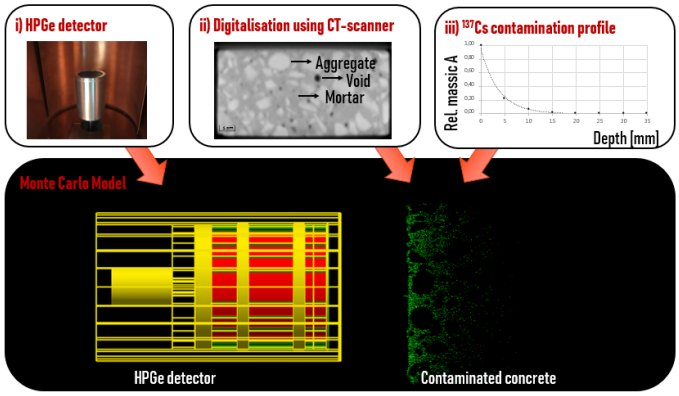

Figure 3. Illustration of the different steps that were performed to create the MC model; i) creating a model of the HPGe detector, ii) making CT scans of the concrete samples, iii) applying different contamination profiles with varying relaxation lengths

IV. RESULTS AND DISCUSSION

Concrete samples were modelled to contain different contamination profiles of ^{137}Cs. In total, ten different concrete samples were scanned. Although all the samples were made with the same mixing recipe, the internal composition per sample is different, as the internal arrangement of voids and aggregates is unique for each sample. The effect of the internal composition on the RLA model is studied by looking at the effect on the FEP efficiency (which is used to calculate the contamination activity) and on the relaxation length (which describes the decrease of contamination with depth).

A. Fluctuations on the FEP efficiency

When applying a contamination profile with a 1/RL value of 0.2 to the different samples, the spectral counts at an energy of 661 keV show deviations that can directly be related to the internal structure. Samples that have more aggregates near the surface of the concrete samples tend to have fewer counts in the peak area, whereas samples that have more mortar (or voids) at the surface lead to more registered counts. This effect is illustrated in Figure 4, where the FEP efficiency at 661 keV of the 10 different spectra are compared to a benchmark situation where a completely homogeneous concrete sample is simulated.

Relative deviations to the FEP efficiency are observed varying from 4% to 9%. For each of the 10 samples, a systematic underestimation of the efficiency would be made when the FEP of the benchmark would be applied. For the X-rays of ^{137}Cs, the relative deviation is even more pronounced as the lower energetic photons are more sensitive to small deviations in the sample density.

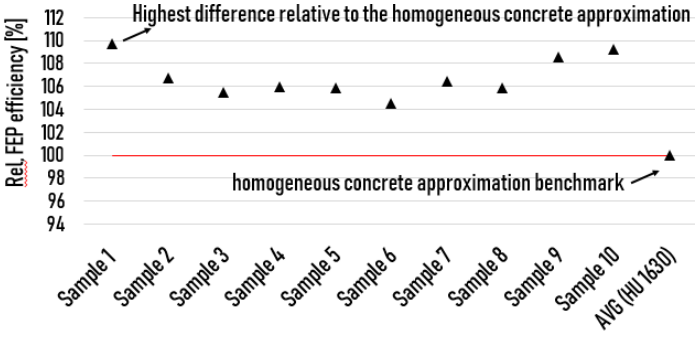

Figure 4. fluctuations of the FEP efficiency of the detector model at 661 keV for 10 different concrete samples. The last data point represents the FEP efficiency of a completely homogeneous concrete sample.

As the FEP efficiency is directly used to calculate the total activity of the contamination, this underestimation would also lead to an erroneous overestimation of the total activity of the contamination. The systematic deviation of the FEP compared to the benchmark can be explained by the density of the concrete near the surface. The top layer of concrete consists of fewer aggregates than the composition of the concrete deeper inside of the samples, leading to an overestimation of the density at the surface.

B. Fluctuations of the relaxation length

Next to the deviations observed for the FEP efficiency (which is used to calculate the source activity), the internal structure will also influence the performance of the RLA model and the corresponding estimation of the relaxation length.

Figure 5 shows the application of the RLA model for 2 extreme situations where i) a concrete sample containing only mortar is simulated and ii) a concrete sample having a density of pure limestone aggregate is simulated for different RL's. These two situations are considered extreme because the densities are respectively the lowest and highest. As a result, the corresponding X-ray to gamma ratio's (which represents the peak area registered in the X-ray peak compared to the peak area of the 661 keV peak) will also represent the boundaries for encountered ratios of more realistic concrete samples as their respective densities lie within the interval constrained by the boundary conditions.

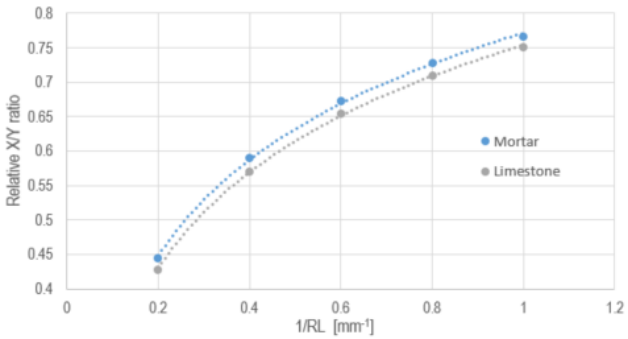

Figure 5. X-ray to gamma intensities for contamination profiles with different RL's relative to a completely planar contamination profile.

The X-ray to gamma ratios are expressed relative to the X-ray to gamma ratios of a completely planar contamination distribution (corresponding to a surface contamination). The ratio increases with increasing 1/RL values. Bigger 1/RL values mean the activity is more concentrated on the surface. In this case, the contamination profile shows a steep decreasing activity with depth and thus resembles pure planar contamination. For 1/RL $\rightarrow$ 0 the relative X-ray to gamma intensity of the contamination profile will match that of a uniform distribution.

As pure limestone is the densest boundary condition, the X-ray to gamma ratio is always lower compared to the ratio of a mortar sample. This is a result of the lower energetic X-rays whose self-attenuation is considerably more sensitive to small changes in density compared to the higher energetic gamma rays.

Figure 5 can be used to determine the maximum error when the density of the concrete sample does not exactly match that of the boundary situations. For example, when an X-ray to gamma ratio of 0.5 is observed (compared to the ratio for a planar source), the matching 1/RL value of the boundary conditions would be 0.258 and 0.284 for respectively mortar and limestone. As a result, the maximum error between both estimations of 1/RL would be approximately 9%. This error can then be used in combination with the error on the FEP efficiency to fully determine the error on the contamination profile and, subsequently, be used to create a decontamination plan.

V. CONCLUSIONS

CT scanning of concrete samples provides valuable insights into the internal structure of concrete. It was demonstrated that CT images can successfully be incorporated into a MC model to study the effects of the internal structure on the RLA model.

By incorporating the internal structure of the 10 concrete samples in the MC model, deviations of up to 9% in the FEP efficiency were observed which are directly linked to the internal structure. The results show that estimations of the FEP efficiency based on a homogeneous concrete sample systematically underestimate the actual FEP efficiency leading to an overestimation of the contamination activity.

For estimating the error on the 1/RL values, an interval described by the boundary conditions defined by pure mortar and limestone samples was determined. The relations between the ratio and the 1/RL can subsequently be used to estimate errors on the 1/RL value when actual concrete samples, consisting of a mixture of mortar and aggregates are measured.

Having quantified the errors on the FEP efficiency and the errors on the determination of 1/RL, a better estimation of the total amount of 'to be removed concrete' material can be made.

VI. REFERENCES

[1] R. Volk, F. Hübner, T. Hünlich, and F. Schultmann, "The future of nuclear decommissioning – A worldwide market potential study," *Energy Policy*, vol. 124, no. August 2018, pp. 226–261, 2019.

[2] Federaal Agenschap voor Nucleaire Controle (FANC), "Kerncentrales in België." [Online]. Available: https://fanc.fgov.be/nl/dossiers/kerncentrales-belgie.

[3] M. Felipe-Sotelo, J. Hinchliff, D. Drury, N. D. M. Evans, S. Williams, and D. Read, "Radial diffusion of radiocaesium and radioiodide through cementitious backfill," *Phys. Chem. Earth*, vol. 70–71, pp. 60–70, 2014.

[4] OECD & NEA, "R&D and Innovation Needs for Decommissioning Nuclear Facilities," 2014.

[5] S. Boden, B. Rogiers, and D. Jacques, "Determination of 137Cs contamination depth distribution in building structures using geostatistical modeling of ISOCS measurements," *Appl. Radiat. Isot.*, vol. 79, pp. 25–36, 2013.

[6] D. Gurau, S. Boden, O. Sima, and D. Stanga, "Determination of the neutron activation profile of core drill samples by gamma-ray spectrometry," *Appl. Radiat. Isot.*, vol. 134, pp. 194–199, Apr. 2018.

[7] SCKCEN, "Customized training courses in decommissioning and decontamination." [Online]. Available: https://www.sckcen.be/en/academy/training-courses/personalized-training-courses/customized-training-courses-decommissioning-and-decontamination.

[8] M. J. Joyce, J. C. Adams, J. A. Heathcote, and M. Mellor, "Finding the depth of radioactivity in construction materials," *Proc. Inst. Civ. Eng. Energy*, vol. 166, no. 2, pp. 67–73, 2013.

[9] International Atomic Energy Agency, "Managing Low Radioactivity Material from the Decommissioning of Nuclear Facilities," 2008.

[10] K. Rybacek, P. Jacob, and R. Meckbach, "In Situ Determination of Deposited Radionuclide Activities : Improved Method Measured Photon Spectra," no. January, 1992.

[11] A. Shippen and M. J. Joyce, "Profiling the depth of caesium-137 contamination in concrete via a relative linear attenuation model," *Appl. Radiat. Isot.*, vol. 68, no. 4–5, pp. 631–634, 2010.

[12] K. M. Miller, P. Shebell, and G. A. Klemic, "In situ gamma-ray spectrometry for the measurement of uranium in surface soils," *Health Phys.*, vol. 67, no. 2, pp. 140–150, 1994.

[13] I. Sato, K. Maeda, M. Suto, M. Osaka, T. Usuki, and S. I. Koyama, "Penetration behavior of water solution containing radioactive species into dried concrete/mortar and epoxy resin materials," *J. Nucl. Sci. Technol.*, vol. 52, no. 4, pp. 580–587, 2015.

[14] K. Maeda *et al.*, "Distribution of radioactive nuclides of boring core samples extracted from concrete structures of reactor buildings in the Fukushima Daiichi Nuclear Power Plant," *J. Nucl. Sci. Technol.*, vol. 51, no. 7–8, pp. 1006–1023, 2014.

[15] L. Brabants, G. Lutter, J. Paepen, B. Vandoren, B. Reniers, and M. Carlo, "Validation of TOPAS MC for modelling the efficiency of an extended-range coaxial p-type HPGe detector," *Appl. Radiat. Isot.*, vol. 173, no. November 2020, 2021.